Embryonic Development of the Cardiovascular System

Wolfgang J. Weninger and Stefan H. Geyer

What You Will Learn in This Chapter
This chapter briefly recapitulates milestones in the morphogenesis of the cardiovascular system. Its focus rests on the development and remodelling of the heart and great arteries.

6.1 Researching Cardiovascular Morphogenesis and Remodelling

For obvious reasons descriptive and experimental research cannot be performed on human embryos. Hence, various biomedical models are used for studying the genetic and biomechanic mechanisms orchestrating the development and remodelling of the cardiovascular system. The chick, frog and zebrafish are mainly employed for unravelling basic genetic decisions and for analysing the influence of biomechanic factors on heart remodelling [6, 14, 17, 21, 22]. Rodents, especially the mouse, are chiefly used for examining the genetic orchestration of normal and pathologic developmental events. They have short reproduction times, and the advancement of molecular tools has reached a level that allows for specific deletion of every single gene of the mouse genome and targeted disruption of gene and gene product function in specific tissues and at specific time points [1, 2, 4, 5, 8, 13, 19].

The advent of sophisticated imaging methods permitting three-dimensional (3D) visualisation of early to late embryos, foetuses and infants of biomedical models in high detail [12, 15, 16, 20, 23, 24] heavily boosted researching the morphogenetic events in cardiovascular development. This chapter will primarily make use of virtual 3D models produced with the high-resolution episcopic microscopy (HREM) technique [11, 18, 25] and traditional wax models produced by Ziegler at the beginning of the twentieth century.

6.2 Early Blood Vessels and Primitive Circulation

In mammals, the formation of the vascular system starts with a process called *vasculogenesis*. Small clusters of haemangioblasts appear in the extraembryonic mesoderm of the yolk sac, body stalk and chorion. They form isolated blood islands and differentiate into endothelial cells surrounding primitive blood cells. Finally, these islands coalesce and form a primitive capillary plexus. In humans this process happens between days 13 and 15 of *intrauterine* development (i.e. end of 4th week of pregnancy) and in the mouse, at approximately embryonic day (E) 8. Around days 15–17, vasculogenesis starts also in the mesoderm inside the embryo, and a plexus of primitive intraembryonal blood vessels forms.

Once a primitive vascular system is shaped, it expands by a process named *angiogenesis*. New, endothelial lined channels sprout from existing vessels, or already established larger channels split after invasion of additional cell material. For details we refer to the chapter "Cellular and Molecular Mechanisms of Vasculogenesis, Angiogenesis, and Lymphangiogenesis".

In human embryos of developmental day 21, the then tubular heart connects to the intra- and extraembryonic vessels. Since it is already pumping, this establishes a primitive unidirectional circulation. First large arteries, the left and right primitive aortae, pass as continuation of the outflow of the tubular heart lateral to the pharynx and turn caudally to descend along the forming intestine. Each dorsal aorta gives rise to segmental arteries, vitelline branches and an umbilical artery. The venous channels are collected by anterior and posterior cardinal veins that enter the cardiac inflow. The components of the primitive

circulatory system undergo dramatic remodelling during the rest of the embryonic period until the foetal circulation is established. The following chapters aim at describing the morphological milestones of these processes in detail.

6.3 Development of the Heart

Even at the beginning of the 2nd week of human *intrauterine* development, cells destined to become heart cells can be identified. At the end of the 3rd week, the embryos have developed a pumping primitive heart then a plump, cranio-caudally arranged tube. This primitive heart tube undergoes complex morphological remodelling in the embryonic period until it has largely achieved its foetal appearance in week 8 of *intrauterine* development. Immediately after birth changes occur in heart morphology to adapt the foetal heart to postnatal requirements.

Correct heart formation and remodelling is essential for sufficient supply of oxygen and nutrients to all the developing organs of the embryo and foetus. Hence an estimated 10% of miscarriages are considered to be a direct result of disrupted embryonic heart development.

6.3.1 Heart Progenitor Cells and First and Second Heart Field

Around the time of implantation into the endometrium, the embryo is composed of two single-cell layers – a dorsal epiblast and a ventral hypoblast. In these early embryos, cell-tracing methods identify cardiac progenitor cells in the epiblast anteriorly to the primitive streak. During gastrulation, which produces the three germ layers ecto-, meso- and endo-derm, these cells and their daughter cells invaginate during mesoderm formation through the primitive streak and end up as parts of the ventral portion of the lateral plate meso-derm, the so-called splanchnic mesoderm.

In the three-layered embryo, the region occupied by the heart progenitor cells is referred to as heart field. As part of the mesoderm, the cells are sandwiched between ento- and ecto-derm and, in the 3rd to 4th week of gestation, are arranged in a horseshoe-shaped, crescent-like structure, the *cardiac crescent*. In mice the two branches of the cardiac crescent are connected anteriorly to the developing neural folds. In humans they are not fused. The lateral area of the branches and the forefront of the cardiac crescent (the toe of the horseshoe) are named as the *first heart field* and the medial part of the branches as the *second heart field*.

6.3.2 Formation of the Linear Heart Tube

On the left and right sides of the embryo, the splanchnic mesoderm of the first heart field forms antero-posteriorly (cranio-caudally) oriented tube-like structures comprised of endothelial (endocardial) cells. Cells of the second heart field are not involved in this process. In the 3rd week, when the most anterior parts of the embryo bend ventrally and form the head fold, these tube-like structures are passively shifted caudally and to the ventral midline. Here they fuse and form a single, very plump primitive heart tube imme-diately ventral to the developing head and foregut. Caudally (posteriorly), two venous channels drain into this tube. Cranially (anteriorly), two primitive ventral aortae leave the
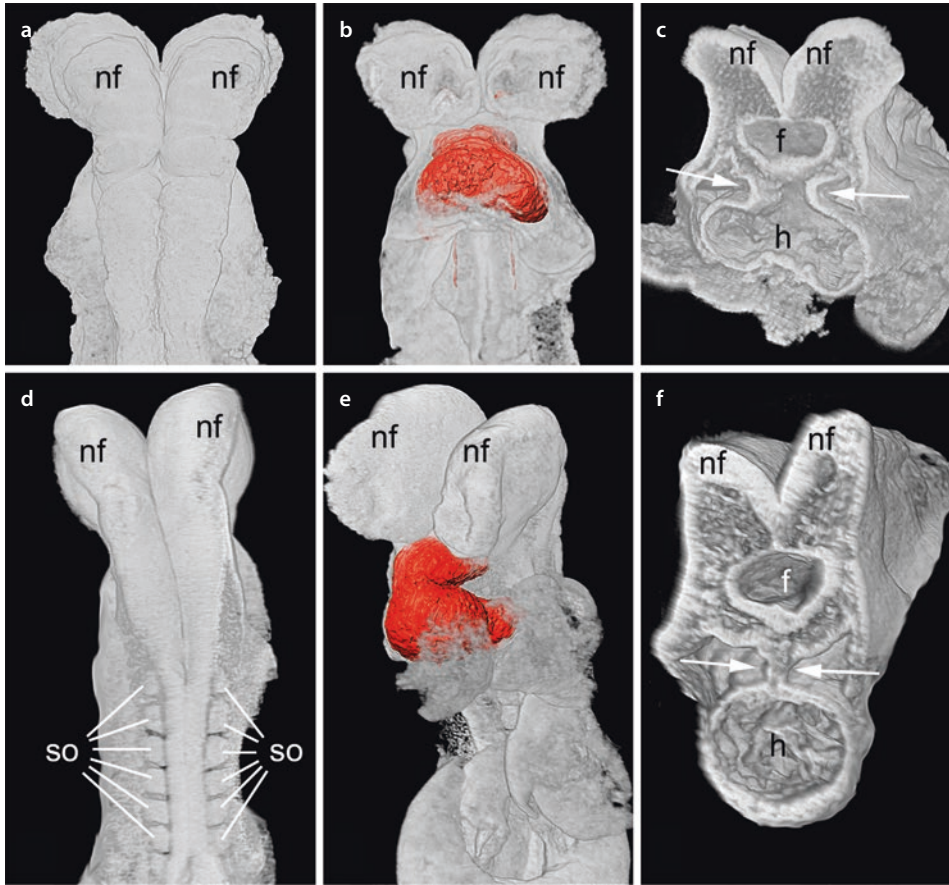
◘ Fig. 6.1 Primitive heart tube. Volume-rendered 3D models of early **a**–**c** and late **d**–**f** mouse embryos of embryonic day (E) 8 and surface-rendered models of their heart tube (red). Models were created out of "high-resolution episcopic microscopy" (HREM) volume data. Anterior (cranial) parts of the embryo from dorsal **a**, **d** and ventral **b**, **e**. Note the plump primitive heart tube and its slender and looped appearance in the later stage. **c**, **f**: Axial sections through the heart region of volume-rendered models. View from anterior. The mesocardium (between arrows) connects the heart tube to the dorsal body wall near the foregut (f). h heart, nf neural fold, so somite

tube (◘ Fig. 6.1). The paired arms of the inflow are destined to become the precursors of the atria, the linear part of the tube transforms to eventually become the left ventricle and the two vessels leaving the outflow are destined to form transitory connections to two primitive aortae developing in the dorsal and caudal parts of the embryo.

The primitive heart tube rests in a cavity, which is termed as the pericardial cavity, although there is no proper pericardium formed yet. It forms at a later time point by migration of cells from the proepicardial organ (see below).

The dorsal aspects of the heart tube are connected to the dorsal wall of the embryo along its foregut region by a meso-like structure called mesocardium (◘ Fig. 6.1). Near the attachment of the mesocardium to the body wall and at the same time laterally to the foregut, the second heart field had been shifted to during head fold formation. From here, cells migrate towards the heart tube and are incorporated into their wall.
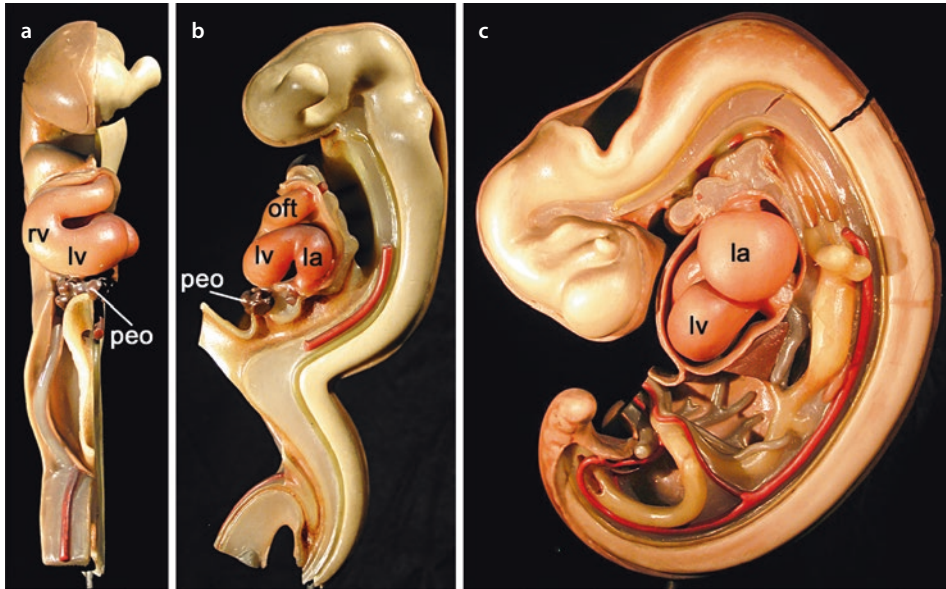
Fig. 6.2 Looping and ballooning. Ziegler wax models of a chick embryo during looping from ventral **a** and left **b**. Note the heart loop and the proepicardial organ (peo). **c** Ballooning of the left atrium (la) and left ventricle (lv). oft outflow tract, rv right ventricle

The lumen of the primitive heart tube is lined with endocardial cells. Myocardial cells appear as if incompletely surrounding the endocardial tube almost as a mantel-like structure. This myocardial mantel layer borders against the pericardial cavity until the epicardium is formed. It does not exist where the mesocardium connects to the heart tube. After forming the mantel layer, the myocardial cells start secreting a complex proteoglycan- and glycosaminoglycan-rich matrix into the space between endocardial and myocardial cells. This matrix, sandwiched between endo- and myocardium, originally does not contain cells and is called *cardiac jelly*.

6.3.3 Looping

After the linear heart tube has formed, cells of the second heart field migrate to it and integrate themselves into its wall. This cell integration quickly leads to a dramatic increase of the length of the heart tube, which is much faster than the cranio-caudal growth of the whole embryo. Therefore, the straight heart tube is forced to assemble a curved shape, and the heart tube starts forming a slender loop protruding into the pericardial cavity. The vertex of the loop points to the right (■ Figs. 6.1 and 6.2).

Elongation of the heart tube is accompanied by disintegration of the mesocardium leaving only the cranial and caudal ends of the heart fixed to the embryonic body tissues. The parts in between the cranial and caudal fixation freely protrude into the pericardial cavity. Consequently, from this time of development, cells, which still migrate from the second heart field and cardiac neural crest towards the heart, can only become associated to the outflow and inflow sections of the heart tube. The cells added to the outflow section form large parts of the later right ventricle and cardiac outflow. The cells added to the

inflow section contribute to the formation of the atria and inflow. Hence, severe heart malformations chiefly affecting the right ventricle and cardiac outflow are often a direct consequence of abnormal migration of cardiac neural crest and/or second heart field cells to the cranial parts of the tubular heart.

In the late looping stages, the future compartments are arranged in a sequential order along the still tubular heart. From caudal to cranial, they are the inflow tract, atrial segment, atrioventricular canal, left ventricle, right ventricle and outflow tract. The outflow tract is connected to the developing pharyngeal arch arteries (◨ Fig. 6.2).

The straight heart has its inflow or venous pole caudally and its outflow or arterial pole cranially. In principle this arrangement remains throughout life, but due to heart elongation and the associated looping and twisting and the growth of the embryo, the relative position of the two poles appears as if having changed after *looping*, with the venous pole being shifted into a dorso-cranial and the arterial pole into an antero-cranial position.

Looping is highly conserved in vertebrates. It is the first feature that makes left-right asymmetry obvious and is governed by molecular signalling cascades, which have been started during gastrulation. Perturbation of these cascades leads to abnormal or left-sided looping and problems in the situs of asymmetric organs. Such laterality defects often are associated with congenital heart defects including serious malformations [17].

6.3.4 Ballooning

The atria and ventricles are formed as pouches that appear at characteristic sites along the heart tube. The pouches grow and expand like balloons, wherefore the whole process of cardiac chamber formation is referred to as *ballooning*, the atria balloon laterally out of the atrial segment of the heart tube and the ventricle balloon in a proximal to distal sequence out of the tube near its vertex (◨ Fig. 6.2).

6.3.4.1 Formation of the Ventricles

During the late phases of heart looping, the mitotic rate locally increases at the outer curvature of the left and right ventricle segments of the cardiac loop. This results in the formation of small thickenings and then of pouches arranged in a proximal to distal sequence along the tube. While the pouches become steadily bigger and start ballooning, the region between them does not significantly change its dimension. As seen from outside, this results in the indentation of an anterior and posterior groove between the ballooning ventricles, the later anterior and posterior interventricular sulcus.

As seen from the heart tube lumen, the ballooning process leads to a local expansion of the lumen at the level of the left and right ventricle segments. The diameter of the lumen in between these two segments does not increase dramatically. Hence the adjacent walls of the two balloons and the material in between form a septum-like structure between the two ventricle cavities. This material is the forerunner of the later muscle part of the *interventricular septum*.

Simultaneously with ballooning of the ventricles, the ventricle myocardium develops two layers: an outer compact tissue layer, with a thickness of 3–4 cardiomyocytes, and an inner layer forming myocardial protrusions into the ventricle cavity that are covered by endocardium. These are called trabeculae carneae. In the early heart, the trabecular layer creates the main contractile force of the developing heart. In addition, the extensions of the ventricle cavities between the trabeculae secure a sufficiently large surface to guarantee smooth supply of oxygen and nutrients to the myocardium until the coronary vasculature is established.

6.3.4.2 Formation of the Atria

In both lateral walls of the singular atrial segment of the heart tube, the mitotic activity increases. This results in the formation of left- and right-sided thickenings and then pouches, which steadily expand until they finally form the appendices of the left and right atrium. These are the forerunner of the later auricula cordis. Inside the appendices myocardial protrusions develop and form pectinate muscles.

The proper atrial spaces are derived from the atrial segment of the heart loop that is located between the atrial appendices and from structures that become secondarily associated with the left and right atrium. The right atrium integrates parts of the sinus venosus, which is the cavity that receives the large systemic veins. The left atrium integrates the vastly expanded space of an originally single pulmonary vein, which receives all four lung veins.

6.3.4.3 Peculiarities of Heart Looping

In contrast to the ventricles, which balloon sequentially from the large curvature of the looping heart, the atrial appendices balloon from its left and right sides. Hence sidedness of the atria is affected by left/right decisions during gastrulation. Consequently, abnormal left/right definition result in abnormal atrium morphology.

An interesting aspect is that elongation of the heart tube during looping is mainly caused by adding cells stemming from the second heart field and cardiac neural crest. In contrast the ballooning process is triggered and maintained by mitoses of cells, which are already part of the cardiac wall.

6.3.5 Epi- and Pericardium

Around the time when heart looping takes place, a vesicular structure formed by mesothelial cells of the septum transversum appears at the base of the sinus venosus. This vesicle is called the *proepicardial organ*. From this organ cells migrate along the cardiac surface and form the epicardium. Cells also migrate along the inside of the pericardial cavity and form the serous layer of the pericardium. A subset of the epicardial cells undergoes *epithelial-mesenchymal transformation*, invades the subepicardial space and forms the subepicardial mesenchyme. These cells also contribute to the formation of the endothelium and smooth muscle cells of the future coronary vessels as well as the forming atrioventricular cushions and valves.

6.3.6 Chamber Separation

6.3.6.1 Atrioventricular Junction

In the looped heart tube, the atrioventricular junction is a relatively long, canal-like segment. A subpopulation of endothelial cells lining this segment undergo endothelial-mesenchymal transformation and invade the cardiac jelly. They stimulate adjacent myocardial cells to produce additional extracellular matrix, which increases the amount of cardiac jelly in the atrioventricular canal and produces two thickenings, the atrioventricular *endocardial cushions*. Because of their position in respect to the orientation of the looped heart tube, these cushions are referred to as superior and inferior atrioventricular cushion. Their size increases until they fuse in the midline, dividing the atrioventricular canal into a left and right portion, the later left and right atrioventricular ostium.

In addition to separating atria and ventricles, the cushion material forms relative thick extensions that protrude into the ventricle cavities and become connected to the trabeculae of the myocardium. After reducing their thickness, these protrusions remain as leaflets of the atrioventricular valves and as chorda tendinea.

6.3.6.2 Atria

In the 5th week of human development, the common space between the left and right atrial appendices starts to become separated into a left and right atrium. In the mouse this happens around E10.5.

After the inflow of the heart has become shifted dorso-cranially during the looping process, muscle tissue starts growing in the midline of the dorso-cranial wall of the atrium into the atrial cavity. This forms the *septum primum*, which at first is crescent-shaped. The space between the free edge of the crescent and the superior atrioventricular cushion (between the left and right atrioventricular ostia) is referred to as *foramen primum*. At the caudal edge of the septum, at the level of the atrioventricular junction, fibrous tissue termed as *spina vestibuli* grows also from dorsal into the atrium. By growing of the septum and spina, the foramen primum becomes gradually smaller and is finally closed with spina vestibuli tissue sandwiched between the atrioventricular cushions and the septum [3]. While the foramen primum closes, parts of the dorsal portion of the septum primum disintegrate, and a foramen opens in the dorsal part, the *foramen secundum*, a forerunner of the *foramen ovale*.

In humans, in the 8th week of intrauterine development (mouse E14), an invagination of the dorso-cranial atrial wall forms a plump ridge right to the septum primum. The ridge is named as *septum secundum* and only extends for a short distance, but far enough to sufficiently cover the foramen secundum in the septum primum (Fig. 6.3).

6.3.6.3 Ventricles

The *interventricular septum* comprises a membranous and a muscular part. First the muscular part is formed by ballooning of the ventricles. Then, during the rest of the embryonic period, its free edge is gradually shifted towards the atrioventricular junction.

The space between the atrioventricular cushions and the free edge of the muscular septum is termed *foramen interventriculare*. It permits blood exchange between the left and right ventricle and persists until the end of the 8th week of gestation (E14.5 in the mouse), which is the beginning of the foetal period. Around this time the muscular portion of the ventricular septum then shifted close to the atrioventricular junction and fuses with a small extension of the atrioventricular cushions, which transforms into the fibrous part of the interventricular septum.

6.3.6.4 Outflow Tract

The cardiac *outflow tract* (conotruncus) has two segments, the proximal *conus arteriosus* and the distal *truncus arteriosus*. The truncus arteriosus continues into the extracardiac *aortic sac*.

During heart looping, the endocardium and the cardiac jelly of the conotruncus form two ridges, twisting like a spiral from proximal to distal. The spiralling arrangement is triggered by haemodynamic forces. Although at this time point the ventricles are connected by an intervertebral foramen, each ventricle pumps a separate stream of blood into the conotruncus, and these blood streams spiral.
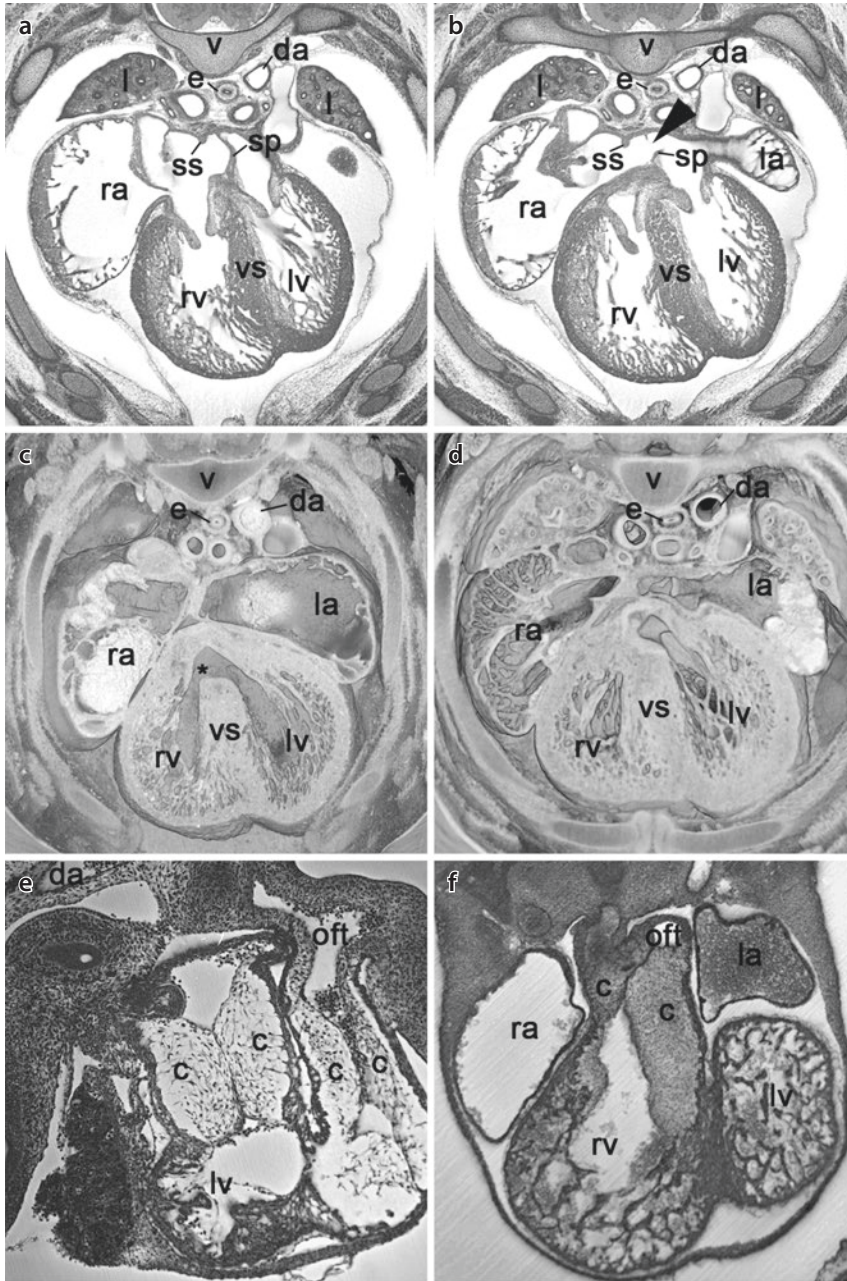
▣ **Fig. 6.3** Separation of chambers and outflow tract. **a**, **b** Atrium septation in an E14.5 mouse embryo. Axial HREM sections through the heart showing septum primum (sp), septum secundum (ss) and foramen secundum (ovale; arrowhead). **c**, **d** Septation of ventricles. Axially sectioned volume-rendered models based on high-resolution episcopic microscopy data viewed from cranial. Early **c** and late E14.5 mouse embryo **d**. Note the interventricular foramen in **c** (asterisk). **e**, **f** Architecture of atrioventricular and outflow tract cushions in a mouse embryo of E10.5 **e** and E12 **f**. c cushion, da descending aorta, e oesophagus, l lung, la left atrium, lv left ventricle, oft outflow tract, ra right atrium, rv right ventricle, sp septum primum, ss septum secundum, v vertebra, vs ventricular septum

Once the ridges are formed, extracardiac cells derived from the neural crest invade the truncal portion of the ridges and trigger the formation of mesenchyme. This causes the ridges to thicken until they fuse, thereby separating the distal outflow tract into two channels, the future aorta and pulmonary trunk. The conal part of the ridges does not receive neural crest cells. Here, cellular material is contributed by endothelial-mesenchymal transformation, which also leads to growing and fusion of the ridges and ultimately to separation of the cardiac outflow.

Nearby the conal parts of the ridges, two small intercalated cushions deriving their mesenchyme mainly by endothelial-mesenchymal transformation are formed. These cushions form the posterior aortic and the anterior pulmonic leaflet of the semilunar valves.

## 6.4 Great Intrathoracic Arteries

Three-week-old embryos have paired dorsal aortae, which descend from the neck to the later lumbar region left and right to the gut-forming entoderm. The lumbar parts of the two aortae fuse to form a single dorsal vessel. Their cranial segments are connected to the heart by primitive aortic arches, which obliterate and vanish after the 1st *pharyngeal arch arteries* are formed (see below) (◘ Fig. 6.4).

Between the 3rd and 6th week of development in humans (E8.5–E13 in mice), the thoracic segments of the dorsal aortae and the ventrally situated aortic sac form buds that grow together and fuse to from six "pairs" of arteries. These arteries appear in a more or less cranio-caudal temporary sequence on both sides of the pharynx and are formed in the mesenchyme of the pharyngeal arches (◘ Fig. 6.4), wherefore they are named as pharyngeal or aortic arch arteries. Immediately after formation, they start to become remodelled. Certain segments are enlarged; others are reduced in diameter or entirely vanish.

At no time point, all six pairs simultaneously exist. For example, most segments of the first two pairs have already largely vanished by the time point the 3rd to 6th are built. Remodelling is largely finished with the start of the foetal period. An exception is the ductus Botalli, which is a derivative of the left 6th pharyngeal arch artery that exists throughout the entire foetal period and obliterates postnatally.

Human embryos only form four pharyngeal (branchial) arches. The material of the 5th and 6th is condensed as the so-called ultimobranchial body. Hence the 5th and 6th pair of pharyngeal arch arteries do not develop inside proper pharyngeal arch mesenchyme but

◘ **Fig. 6.4**   Pharyngeal arch arteries. **a**–**c** Ziegler wax models of chick embryos. View from right of subsequent developmental stages. Right primitive aortic arch (rpaa) and right pharyngeal arch arteries 1 (r1)–4 (r4). **d**–**i**. Surface-rendered 3D models of the pharyngeal arch arteries of mouse embryos between embryonic day (E)12 **d**–**f** and E12.5 **g**–**i** derived from HREM volume data. View from right **d**, **g**, ventral **e**, **h** and left **f**, **i**. Note the not yet fully separated ascending aorta (aa) and pulmonary trunk (pt) in **d**–**f**. bt brachiocephalic trunk, da descending aorta, h heart, lc left common carotid artery, ldoa left dorsal aorta, ls left subclavian artery, l3 left 3rd pharyngeal arch artery, l4 left 4th pharyngeal arch artery, l5 left 5th pharyngeal arch artery, l6 left 6th pharyngeal arch artery, pa pulmonary artery, rav right anterior cardinal vein, rc right common carotid artery, rdoa right dorsal aorta, rpv right posterior cardinal vein, rs right subclavian artery, r1 right 1st pharyngeal arch artery, r2 right 2nd pharyngeal arch artery, r3 right 3rd pharyngeal arch artery, r4 right 4th pharyngeal arch artery, r6 right 6th pharyngeal arch artery, 3 3rd pharyngeal arch artery, 4 4th pharyngeal arch artery, 5 5th pharyngeal arch artery, 6 6th pharyngeal arch artery

Embryonic Development of the Cardiovascular System
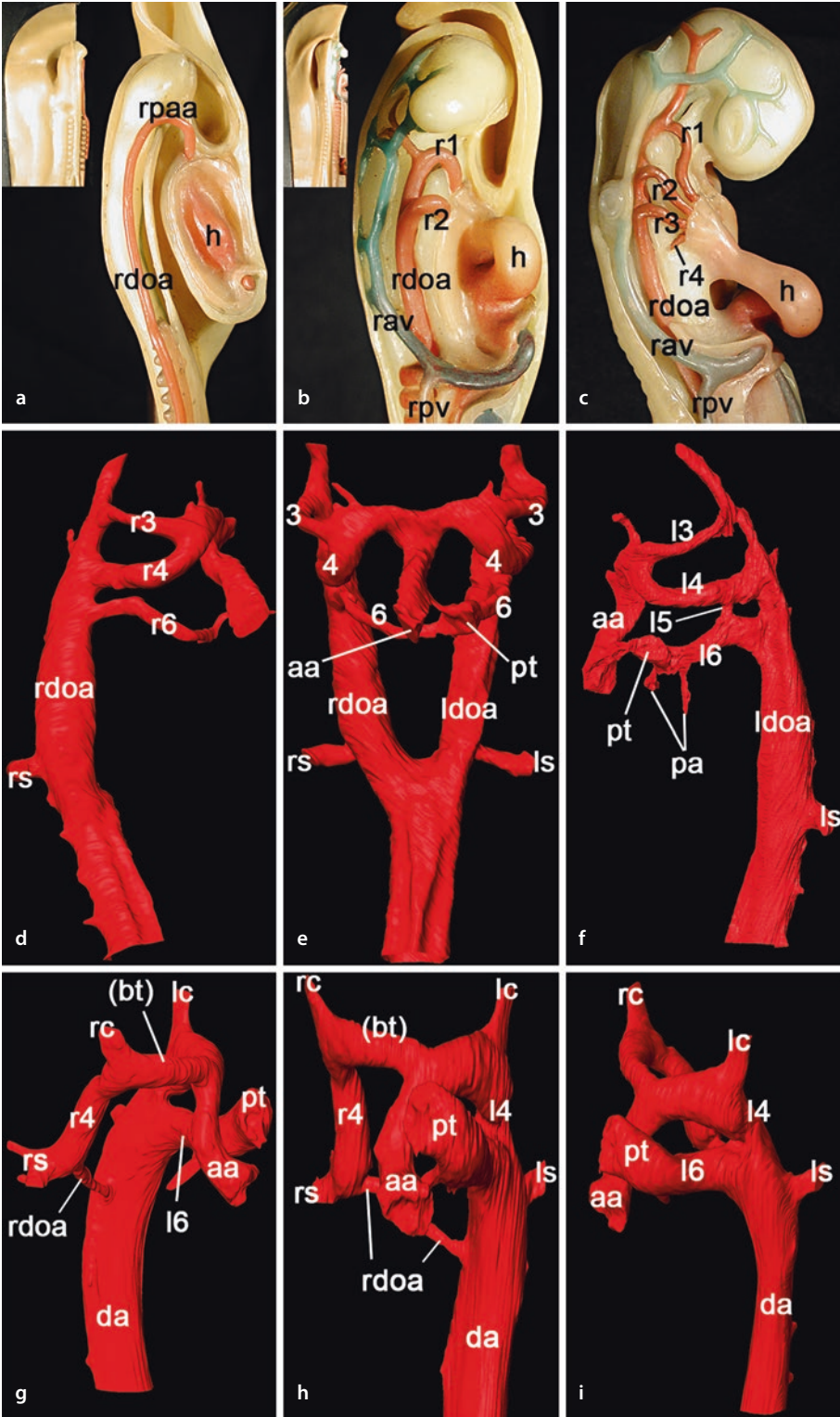
in the mesenchyme laterally to the ultimobranchial body. This has a peculiar effect on the 5th and 6th pair. The 5th pair forms after the 6th pair is already established and shows up as a connection between the 4th and 6th pharyngeal arch arteries, which runs in parallel to the segment of the dorsal aorta between the 4th and 6th pharyngeal arch arteries with a branch sometimes connecting to this segment [7, 9, 10] (◘ Fig. 6.4).

Segments of the first and second pair of pharyngeal arch arteries are remodelled to become segments of head arteries, while the 3rd to 6th are remodelled into the great intrathoracic arteries. From the first pharyngeal arch artery, material only remains as segments of the *maxillary artery* and the *external carotid artery*. Material from the distal portion of the 2nd pharyngeal arch artery forms the *stapedial artery*, which is the main source of blood supply to the orbit in rodents, but a transient embryonic vessel in humans. Hence, from the foetal stages onwards, there are no derivatives of the second pharyngeal arch arteries.

The 3rd to 6th pairs of pharyngeal arch arteries remodel to form the unpaired aortic arch and the great intrathoracic arteries of the foetal cardiovascular system. The remodelling process is highly complex and influenced by haemodynamic forces and cardiac neural crest cells. At the time point the pharyngeal arch arteries start forming, the latter migrate in the mesenchyme of the forming pharyngeal arches towards the outflow tract of the heart. Some remain in the mesenchyme and become incorporated into the walls of the pharyngeal arch arteries.

Material of pharyngeal arch arteries three to six contributes to the following foetal blood vessels: Segments of the third pharyngeal arch arteries remain as parts of the *common carotid* and proximal parts of *internal carotid arteries*. Segments of the left 4th pharyngeal arch artery remain as the segment of the aortic arch between left common carotid and left subclavian artery (the proximal part of the aortic arch develops from the aortic sac and primitive ventral aorta). The right 4th pharyngeal arch artery remains as the proximalmost segment of the right subclavian artery. The 5th pair of pharyngeal arch arteries exists only transiently and vanishes entirely. The left 6th pharyngeal arch artery contributes to the distal pulmonary trunk and persists as *ductus arteriosus (Botalli)*. The latter is essential for foetal circulation and obliterates postnatally. The proximal part of the right 6th pharyngeal arch artery persists as the most proximal part of the right pulmonary artery (◘ Table 6.1 and ◘ Fig. 6.5).

The segments of the left and right dorsal aorta in between the pharyngeal arch arteries obliterate and vanish, except for the segment between the left 4th and 6th pharyngeal arch arteries. This segment seems to remain as a very small part of the aortic arch proximal to the origin of the left subclavian artery. The segment of the right dorsal aorta between the 6th pharyngeal arch artery and the bifurcation where the two dorsal aortae form a single vessel first elongates and then obliterates and vanishes immediately before the foetal circulation is established.

Abnormal remodelling, that is, abnormal regression or persistence of single pharyngeal arch arteries, is quite frequent. Examples are double lumen aortic arch as persistence of the left 5th pharyngeal arch artery, type B interrupted aortic arch as a result of total regression of the left 4th pharyngeal arch artery and retro-oesophageal right subclavian artery, as an example of abnormally total regression of the right 4th pharyngeal arch artery (◘ Fig. 6.5).

6.5   Foetal Circulation

The foetus swims in the amnion and lacks the ability to eat or breath. It therefore receives nutrients and oxygen via the placenta. The placenta is an organ comprised of maternal and foetal material, in which foetal blood vessels directly border to maternal blood spaces.

| ▣ Table 6.1 Derivatives of pharyngeal arch arteries (PAA)	
PAA	**Derivatives**
1st	Segments of maxillary artery
	Ventral part of external carotid artery
2nd	Stapedial artery
3rd	Distal segment of common carotid artery
	Proximal segment of internal carotid artery
Right 4th	Proximal segment of right subclavian artery
Left 4th	Aortic arch between left carotid and left subclavian artery
5th	–
Right 6th	Proximal pulmonary artery
Left 6th	Distal pulmonary trunk
	Ductus arteriosus Botalli

Small substances, up to a molecular weight of 1000 Da, can diffuse through the so-called placental barrier from the maternal into the foetal blood and vice versa.

From the placenta the umbilical vein brings blood back to the foetus. It runs in the umbilical cord, enters the foetal body through the navel and continues in the free lower rim of the ventral mesogastrium towards the liver hilus. Here it drains into the left branch of the portal vein. In contrast to the foetus, embryos have a left and right umbilical vein. But most segments of the right umbilical vein obliterate during embryogenesis leaving only a thin vessel, the paraumbilical vein that connects the subcutaneous veins of the body wall with the liver vasculature. Even this remnant of the right umbilical vein often fully obliterates during the foetal period.

From the left branch of the portal vein, a thick blood channel, the *ductus venosus* (Arantii), arises and connects to the vena cava inferior. The vena cava inferior pierces the diaphragm, enters the pericardial cavity and drains into the right atrium from caudal. Thus, the vast majority of the oxygenated blood entering the portal vein circumvents the liver vasculature via the ductus venosus and almost directly reaches the foetal heart. Only small amounts of oxygenated blood enter the liver. Since the foetal heart pumps the foetal circulation and the blood flow is from the placenta to the heart, all these vessels are veins.

In the right atrium, at the ostium of the vena cava inferior, a valvelike structure, the valva venae cavae inferioris (Eustachii) directs the blood stream directly towards the foramen ovale. On its way it passes to the almost canal-like space left to the septum secundum and the free edge of the septum primum, thereby bulging the septum primum leftwards into the cavity of the left atrium. Thus, the oxygenated blood enters the left atrium through the foramen ovale (former foramen secundum) in a caudo-cranial direction. Once in the left atrium, the relatively high pressure in the lung veins prevents the blood from draining into these veins, and it takes its way through the left atrioventricular ostium into the left ventricle.

The left ventricle pumps blood into the aorta. Through the coronary arteries, it supplies oxygen and nutrients to the heart and through the big arteries of the aortic arch to both

6
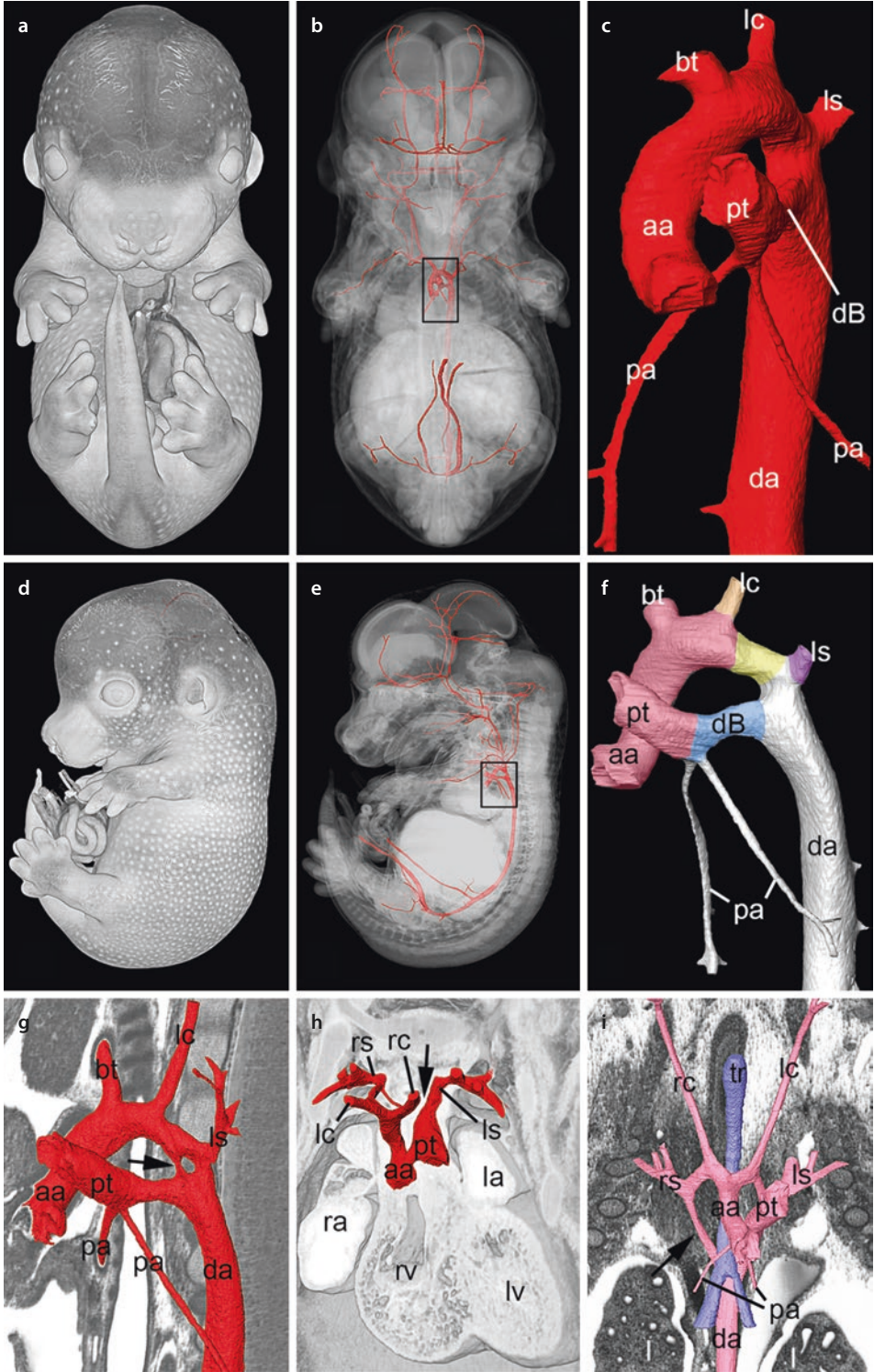
upper limbs and the head and neck. The rest of the oxygenated blood enters the descending aorta and mixes with the low-oxygen blood coming through the ductus arteriosus.

The venous blood from the upper body comes back to the heart via the veins collected by the superior vena cava. It enters the right atrium from cranial. Inside the atrium the blood stream passes ventrally to the stream of blood from the vena cava inferior almost without mixing. Through the right atrioventricular ostium, it then enters the right ventricle, which pumps it into the truncus pulmonalis. Since the lung is not yet inflated, the high pressure inside the lung vasculature forces the majority of the low-oxygen blood to take its way through the ductus arteriosus into the descending aorta. Thus the first segment of the descending aorta receives oxygenated blood through the aortic arch and low-oxygen (venous) blood via the ductus arteriosus.

The descending aorta gives rise to intercostal arteries, transits the diaphragm and supplies blood to the abdominal and retroperitoneal organs. It bifurcates into the common iliac arteries. Each common iliac artery in turn bifurcates into an internal and external iliac artery, which supply blood to the pelvic organs and lower limbs. The first branch of the left and right internal iliac artery is the umbilical artery. The two umbilical arteries ascend towards the navel and, running inside the umbilical cord, take the low-oxygen (venous) blood back to the placenta.

Blood from the lower body half is collected by vessels draining into the vena cava inferior or to a small amount into the azygos vein, which drains into the vena cava superior. Venous blood from the gut drains into the portal vein and either enters the liver vasculature or to a very small amount is taken into the ductus venosus, together with the oxygenated blood coming via the umbilical vein.

■ **Sites at Which Arterious and Venous Blood Mix**

The foetal circulation has some sites where blood with high and low oxygen levels mix up:

1. Left branch of portal vein

   The portal vein and thus also its left branch receive blood from the gut. But the left branch also receives the umbilical vein and opposite to its junction gives rise to the ductus venosus. Hence, small amounts of oxygenated blood coming with the umbilical vein and low-oxygen blood coming from the gut mix up at this crossroad.

2. Connection inferior vena cava/ductus venosus

   The vena cava inferior receives venous blood from the lower body. This becomes mixed into the oxygenated blood draining into the vena cava inferior through the ductus venosus.

◘ **Fig. 6.5** Foetal arrangement of great intrathoracal arteries (E14.5 mouse foetus). **a–f** Volume-rendered and surface-rendered 3D models reconstructed from "high-resolution episcopic microscopy" (HREM). **c** and **f** enlargement of arteries in the boxed region of **b** and **e**. View from ventral **a–c** and from left **d–f**. Colour coding in **f** indicates the derivation of the segments of the great arteries from the respective pharyngeal arch arteries. Aortic sac (red), left 3rd pharyngeal arch artery (orange), left 4th pharyngeal arch artery (yellow), left subclavian artery (violet) and left 6th pharyngeal arch artery (blue). **g–h** Examples of malformations caused by abnormal remodelling of the pharyngeal arch arteries. **g** Double lumen aortic arch. Arrow points to remnant of 5th pharyngeal arch artery. **h** Interrupted aortic arch type B. Arrow points to position of missing segment of left 4th pharyngeal arch artery. I. Persisting right dorsal aorta (arrow). aa ascending aorta, bt brachiocephalic trunk, da descending aorta, dB ductus arteriosus Botalli, l lung, la left atrium, lc left common carotid artery, ls left subclavian artery, lv left ventricle, pa pulmonary artery, pt pulmonary trunk, ra right atrium, rc right common carotid artery, rs right subclavian artery, rv right ventricle, tr trachea

3. Connection liver veins/inferior vena cava

   Between the connection with the ductus venosus and it draining into right atrium, the vena cava inferior receives the liver veins. They mix low-oxygen blood draining from the liver into the oxygenated blood of the vena cava inferior.

4. Right atrium

   The anterior space of the right atrium receives low-oxygen blood via the superior vena cava and the coronary sinus. The posterior part receives oxygenated blood via the inferior vena cava, which is directed towards the foramen ovale by the valva Eustachii. Most of the time, the two blood streams pass through the atrium, one ventrally and one dorsally, without much interference. But during atrium contraction, small amounts of oxygen-rich and oxygen-poor blood get mixed.

5. Left atrium

   The left atrium receives oxygenated blood through the foramen ovale. Low-oxygen blood enters from the four lung veins. Since the lungs are not inflated yet, this is only a small amount.

6. Connection ductus arteriosus/descending aorta

   From the aorta oxygenated blood drains into the descending aorta. Low-oxygen blood comes via the ductus arteriosus.

> **Take-Home Message**
>
> Detailed descriptions of cardiovascular morphogenesis and profound knowledge of the genetic and biomechanic factors triggering and orchestrating each single step and event are essential for understanding cardiovascular malformations and diseases.

References

1. Abu-Issa R, Smyth G, Smoak I, Yamamura K, Meyers EN. Fgf8 is required for pharyngeal arch and cardiovascular development in the mouse. Development. 2002;129(19):4613–25.
2. Andelfinger G. Genetic factors in congenital heart malformation. Clin Genet. 2008;73(6):516–27.
3. Anderson RH, Webb S, Brown NA, Lamers W, Moorman A. Development of the heart: (2) Septation of the atriums and ventricles. Heart. 2003;89(8):949–58.
4. Anderson GA, Udan RS, Dickinson ME, Henkelman RM. Cardiovascular patterning as determined by hemodynamic forces and blood vessel genetics. PLoS One. 2015;10(9):e0137175. https://doi.org/10.1371/journal.pone.0137175.
5. Ayadi A, Birling MC, Bottomley J, Bussell J, Fuchs H, Fray M, Gailus-Durner V, Greenaway S, Houghton R, Karp N, Leblanc S, Lengger C, Maier H, Mallon AM, Marschall S, Melvin D, Morgan H, Pavlovic G, Ryder E, Skarnes WC, Selloum M, Ramirez-Solis R, Sorg T, Teboul L, Vasseur L, Walling A, Weaver T, Wells S, White JK, Bradley A, Adams DJ, Steel KP, Hrabe de Angelis M, Brown SD, Herault Y. Mouse large-scale phenotyping initiatives: overview of the European Mouse Disease Clinic (EUMODIC) and of the Wellcome Trust Sanger Institute Mouse Genetics Project. Mamm Genome. 2012;23(9–10):600–10. https://doi.org/10.1007/s00335-012-9418-y.
6. Baldessari D, Mione M. How to create the vascular tree? (Latest) help from the zebrafish. Pharmacol Ther. 2008;118(2):206–30. https://doi.org/10.1016/j.pharmthera.2008.02.010.
7. Bamforth SD, Chaudhry B, Bennett M, Wilson R, Mohun TJ, Van Mierop LH, Henderson DJ, Anderson RH. Clarification of the identity of the mammalian fifth pharyngeal arch artery. Clin Anat. 2013;26(2):173–82. https://doi.org/10.1002/ca.22101.
8. Brown CB, Wenning JM, Lu MM, Epstein DJ, Meyers EN, Epstein JA. Cre-mediated excision of Fgf8 in the Tbx1 expression domain reveals a critical role for Fgf8 in cardiovascular development in the mouse. Dev Biol. 2004;267(1):190–202.

9. Geyer SH, Weninger WJ. Some mice feature 5th pharyngeal arch arteries and double-lumen aortic arch malformations. Cells Tissues Organs. 2012;196:90–8. https://doi.org/10.1159/000330789.. 000330789 [pii].

10. Geyer SH, Weninger WJ. Metric characterization of the aortic arch of early mouse fetuses and of a fetus featuring a double lumen aortic arch malformation. Ann Anat. 2013;195(2):175–82. https://doi.org/10.1016/j.aanat.2012.09.001.. S0940-9602(12)00139-2 [pii].

11. Geyer SH, Reissig LF, Husemann M, Hofle C, Wilson R, Prin F, Szumska D, Galli A, Adams DJ, White J, Mohun TJ, Weninger WJ. Morphology, topology and dimensions of the heart and arteries of genetically normal and mutant mouse embryos at stages S21-S23. J Anat. 2017;231(4):600–14. https://doi.org/10.1111/joa.12663.

12. Handschuh S, Beisser CJ, Ruthensteiner B, Metscher BD. Microscopic dual-energy CT (microDECT): a flexible tool for multichannel ex vivo 3D imaging of biological specimens. J Microsc. 2017. https://doi.org/10.1111/jmi.12543.

13. Kelly RG, Buckingham ME, Moorman AF. Heart fields and cardiac morphogenesis. Cold Spring Harb Perspect Med. 2014;4(10):a015750. https://doi.org/10.1101/cshperspect.a015750.

14. Linask KK, Yu X, Chen Y, Han MD. Directionality of heart looping: effects of Pitx2c misexpression on flectin asymmetry and midline structures. Dev Biol. 2002;246(2):407–17. https://doi.org/10.1006/dbio.2002.0661.. S0012160602906615 [pii].

15. Liu X, Tobita K, Francis RJ, Lo CW. Imaging techniques for visualizing and phenotyping congenital heart defects in murine models. Birth Defects Res C Embryo Today. 2013;99(2):93–105. https://doi.org/10.1002/bdrc.21037.

16. Liu M, Maurer B, Hermann B, Zabihian B, Sandrian MG, Unterhuber A, Baumann B, Zhang EZ, Beard PC, Weninger WJ, Drexler W. Dual modality optical coherence and whole-body photoacoustic tomography imaging of chick embryos in multiple development stages. Biomed Opt Express. 2014;5(9):3150–9. https://doi.org/10.1364/boe.5.003150.

17. Männer J. The anatomy of cardiac looping: a step towards the understanding of the morphogenesis of several forms of congenital cardiac malformations. Clin Anat. 2009;22(1):21–35. https://doi.org/10.1002/ca.20652.

18. Mohun TJ, Weninger WJ. Imaging heart development using high-resolution episcopic microscopy. Curr Opin Genet Dev. 2011;21(5):573–8. https://doi.org/10.1016/j.gde.2011.07.004.. S0959-437X(11)00111-0 [pii].

19. Moon AM. Mouse models for investigating the developmental basis of human birth defects. Pediatr Res. 2006;59(6):749–55. https://doi.org/10.1203/01.pdr.0000218420.00525.98.

20. Norris FC, Wong MD, Greene ND, Scambler PJ, Weaver T, Weninger WJ, Mohun TJ, Henkelman RM, Lythgoe MF. A coming of age: advanced imaging technologies for characterising the developing mouse. Trends Genet. 2013;29(12):700–11. https://doi.org/10.1016/j.tig.2013.08.004.

21. Ribeiro I, Kawakami Y, Buscher D, Raya A, Rodriguez-Leon J, Morita M, Rodriguez Esteban C, Izpisua Belmonte JC. Tbx2 and Tbx3 regulate the dynamics of cell proliferation during heart remodeling. PLoS One. 2007;2(4):e398. https://doi.org/10.1371/journal.pone.0000398.

22. Swift MR, Weinstein BM. Arterial-venous specification during development. Circ Res. 2009;104(5):576–88. https://doi.org/10.1161/CIRCRESAHA.108.188805.

23. Tobita K, Liu X, Lo CW. Imaging modalities to assess structural birth defects in mutant mouse models. Birth Defects Res C Embryo Today. 2010;90(3):176–84. https://doi.org/10.1002/bdrc.20187.

24. Weninger WJ, Geyer SH, Mohun TJ, Rasskin-Gutman D, Matsui T, Ribeiro I, Costa Lda F, Izpisua-Belmonte JC, Müller GB. High-resolution episcopic microscopy: a rapid technique for high detailed 3D analysis of gene activity in the context of tissue architecture and morphology. Anat Embryol. 2006;211(3):213–21.

25. Weninger WJ, Geyer SH, Martineau A, Galli A, Adams DJ, Wilson R, Mohun TJ. Phenotyping structural abnormalities in mouse embryos using high-resolution episcopic microscopy. Dis Model Mech. 2014;7(10):1143–52. https://doi.org/10.1242/dmm.016337.. 7/10/1143 [pii].